


Tracing Isomanifolds in \mathbb{R}^d in Time Polynomial in d Using Coxeter-Freudenthal-Kuhn Triangulations

Jean-Daniel Boissonnat ✉

Université Côte d'Azur, Inria, Sophia-Antipolis, France

Siargey Kachanovich ✉

Université Côte d'Azur, Inria, Sophia-Antipolis, France

Mathijs Wintraecken ✉ 

IST Austria (Institute of Science and Technology Austria), Klosterneuburg, Austria

Abstract

Isomanifolds are the generalization of isosurfaces to arbitrary dimension and codimension, i.e. submanifolds of \mathbb{R}^d defined as the zero set of some multivariate multivalued smooth function $f : \mathbb{R}^d \rightarrow \mathbb{R}^{d-n}$, where n is the intrinsic dimension of the manifold. A natural way to approximate a smooth isomanifold \mathcal{M} is to consider its Piecewise-Linear (PL) approximation $\hat{\mathcal{M}}$ based on a triangulation \mathcal{T} of the ambient space \mathbb{R}^d . In this paper, we describe a simple algorithm to trace isomanifolds from a given starting point. The algorithm works for arbitrary dimensions n and d , and any precision D . Our main result is that, when f (or \mathcal{M}) has bounded complexity, the complexity of the algorithm is polynomial in d and $\delta = 1/D$ (and unavoidably exponential in n). Since it is known that for $\delta = \Omega(d^{2.5})$, $\hat{\mathcal{M}}$ is $O(D^2)$ -close and isotopic to \mathcal{M} , our algorithm produces a faithful PL-approximation of isomanifolds of bounded complexity in time polynomial in d . Combining this algorithm with dimensionality reduction techniques, the dependency on d in the size of $\hat{\mathcal{M}}$ can be completely removed with high probability. We also show that the algorithm can handle isomanifolds with boundary and, more generally, isostratifolds. The algorithm for isomanifolds with boundary has been implemented and experimental results are reported, showing that it is practical and can handle cases that are far ahead of the state-of-the-art.

2012 ACM Subject Classification Theory of computation \rightarrow Computational geometry

Keywords and phrases Coxeter triangulation, Kuhn triangulation, permutahedron, PL-approximations, isomanifolds/solution manifolds/isosurfacing

Digital Object Identifier 10.4230/LIPIcs.SoCG.2021.17

Related Version *Full Version:* <https://hal.archives-ouvertes.fr/hal-03006663>

Funding The research leading to these results has received funding from the European Research Council (ERC) under the European Union's Seventh Framework Programme (FP/2007-2013) / ERC Grant Agreement No. 339025 GUDHI (Algorithmic Foundations of Geometry Understanding in Higher Dimensions).

Jean-Daniel Boissonnat: Supported by the French government, through the 3IA Côte d'Azur Investments in the Future project managed by the National Research Agency (ANR) with the reference number ANR-19-P3IA-0002.

Mathijs Wintraecken: Supported by the European Union's Horizon 2020 research and innovation programme under the Marie Skłodowska-Curie grant agreement No. 754411.

Acknowledgements We thank Dominique Attali, Guilherme de Fonseca, Arijit Ghosh, Vincent Pilaud and Aurélien Alvarez for their comments and suggestions. We also acknowledge the reviewers.



© Jean-Daniel Boissonnat, Siargey Kachanovich, and Mathijs Wintraecken; licensed under Creative Commons License CC-BY 4.0

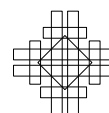
37th International Symposium on Computational Geometry (SoCG 2021).

Editors: Kevin Buchin and Éric Colin de Verdière; Article No. 17; pp. 17:1–17:16

Leibniz International Proceedings in Informatics



LIPICs Schloss Dagstuhl – Leibniz-Zentrum für Informatik, Dagstuhl Publishing, Germany



1 Introduction

Given a surface represented in \mathbb{R}^3 as the zero set of a function $f : \mathbb{R}^3 \rightarrow \mathbb{R}$, the goal of isosurfacing is to find a piecewise linear (PL) approximation of the surface. This question naturally extends to isomanifolds of higher dimensions and codimensions defined as the zero set of multivariate multivalued smooth functions $f : \mathbb{R}^d \rightarrow \mathbb{R}^{d-n}$. Isosurfaces play a crucial role in medical imaging, computer graphics and geometry processing [22]. Higher dimensional isomanifolds are also of fundamental importance in many fields like statistics [10], dynamical systems [25], econometrics, or mechanics [22].

State-of-the-art. The most widely used algorithm to trace isomanifolds is the Marching Cube (MC) algorithm and its numerous variants [17, 27]. The MC algorithm uses a cubical grid to tessellate the ambient space. In many applications in 3-dimensions, the ambient space is decomposed into unstructured tetrahedral meshes, which led to the development of a variant of the MC algorithm named the Marching Tetrahedra algorithm. In higher dimensions, any tessellation of the ambient space has a complexity that depends exponentially on the ambient dimension. Hence a key to extending marching algorithms to higher dimensions is to circumvent the curse of dimensionality by using an *implicit* representation of the ambient tessellation. This is impossible for general triangulations but easy to do if one uses a grid. However, using a grid has other drawbacks and is not sufficient to break the exponential barrier. The reason for this is that the number of configurations inside a cubical cell grows exponentially with the dimension [27].

Hence the most promising approach seems to be to subdivide the ambient space \mathbb{R}^d using a highly regular triangulation such as the Freudenthal-Kuhn triangulation. Some early work along this direction has been published in Applied Mathematics [2, 15, 25], and a slightly more recent paper by Dobkin et al. [13] attracted the interest of the Computer Graphics community to the related Coxeter triangulations. Dobkin et al. however only considered the case of curves ($n = 1$). The most advanced work we are aware of is due to Min [21]. Min's method uses the Freudenthal-Kuhn triangulation over a dyadic grid of \mathbb{R}^d and applies to isomanifolds of any dimension and codimension. The time complexity of Min's method is, with our notations, $O(\delta^n \log \delta)$, where $\delta = 1/D$ and D is the maximal diameter of the simplices. The ambient dimension d is a constant hidden in the big O . The fact that the exponent of δ is the intrinsic dimension n , and not the ambient dimension d is a clear improvement over earlier methods. However, although not explicitly analysed by Min, the complexity in d remains exponential, and the method seems to be limited to small ambient dimensions. Experimental results are only reported in 3, and 4D.

Contributions. This paper discusses an efficient algorithm to compute a PL-approximation of isomanifolds. We extend the work of Dobkin et al. [13] and describe a simple algorithm to trace an n -dimensional isomanifold \mathcal{M} of \mathbb{R}^d for arbitrary n and d . Our algorithm uses any triangulation of a family of regular triangulations of \mathbb{R}^d that includes the Coxeter and the Freudenthal-Kuhn triangulations. Contrary to Min [21], our results are obtained with a uniform triangulation leading to a very simple algorithm. Key to our results, is a data structure that can implicitly store the full facial structure of such triangulations. The data structure is very compact and allows to retrieve the faces or the cofaces of a simplex of any dimension in an output sensitive way. Using this data structure, one can trace a connected submanifold of \mathbb{R}^d , starting from a given initial point on the manifold (Section 3). Our algorithm produces a PL-approximation of size polynomial in d and $\delta = 1/D$, and exponential in n . The complexity of the algorithm is also polynomial in d , and δ , and exponential in n .

Moreover, by taking δ large enough, the PL-approximation output by the algorithm is a faithful approximation of the isomanifold. Specifically, as shown in the full version of [9] and recalled in Section 2.2, if we take $\delta = \Omega(d^{2.5})$, the PL-approximation $\hat{\mathcal{M}}$ is $O(D^2)$ -close and isotopic to the isomanifold. Here the constants in the O depend on f and its derivatives. Hence, our algorithm constructs geometrically close and topologically correct PL-approximation of isomanifolds of bounded complexity in polynomial time.

Our algorithm can be extended in several directions. First, the dependency on d in the size of $\hat{\mathcal{M}}$ can be completely removed by combining our algorithm with dimensionality reduction (Section 3.4). We can also extend the algorithm to the case of isomanifolds with boundary and, more generally, to stratifolds (Section 3.5).

The algorithm has been implemented. In Section 4, we report on experimental results which show that the algorithm is practical and can handle cases that are far 16 ahead of the state-of-the-art. We also present an application in Algebraic Geometry that was used to verify a conjecture on projective varieties defined by polynomial equations in the complex projective plane. Following numerous experiments on various projective varieties, the conjecture was ultimately proved by Alvarez and Deroin [4].

The approximation of a manifold that is the zero set of a function is an example of the more general question of how to triangulate a manifold which has a long history in Mathematics. In particular, Whitney [28] introduced a construction that has some similarity with the present algorithm (see [7]). A major difference though is that topological guarantees can only be obtained if some intricate perturbations of the ambient triangulation are performed (Section 5). These techniques are at the moment incompatible with polynomial complexity.

2 Background

2.1 Permutahedral representation of CFK-triangulations

In this section, we give the most important definitions and basic properties of Coxeter and Freudenthal-Kuhn triangulations. An extensive discussion can be found in [8, Appendix A].

Both Coxeter and Freudenthal-Kuhn triangulations can be described as an arrangement of hyperplanes. They are related by an affine transformation. Let E be a finite set of vectors of \mathbb{R}^d and consider the set of hyperplanes $H_E = \{x \in \mathbb{R}^d \mid \langle x, u \rangle = k, u \in E, k \in \mathbb{Z}\}$. Let, in addition, H be the hyperplane of \mathbb{R}^{d+1} of equation $\langle x, \mathbf{1} \rangle = 0$ where $\mathbf{1}$ is the vector of \mathbb{R}^{d+1} whose coordinates are all 1.

► **Definition 1.** *The Freudenthal-Kuhn triangulation is the hyperplane arrangement $\mathcal{H}_{E_{FK}}$ associated to the set of vectors $E_{FK} = \{e_1, \dots, e_d\} \cup \{u_{i,j} = e_j - e_i \mid 1 \leq i < j \leq d\}$. The Coxeter triangulation of type \tilde{A}_d is the hyperplane arrangement \mathcal{H}_{E_C} in \mathbb{R}^{d+1} associated to the set of vectors $E_C = \{r_{i,j} = e_i - e_{j+1} \mid 1 \leq i \leq j \leq d\}$, restricted to $H \simeq \mathbb{R}^d$.*

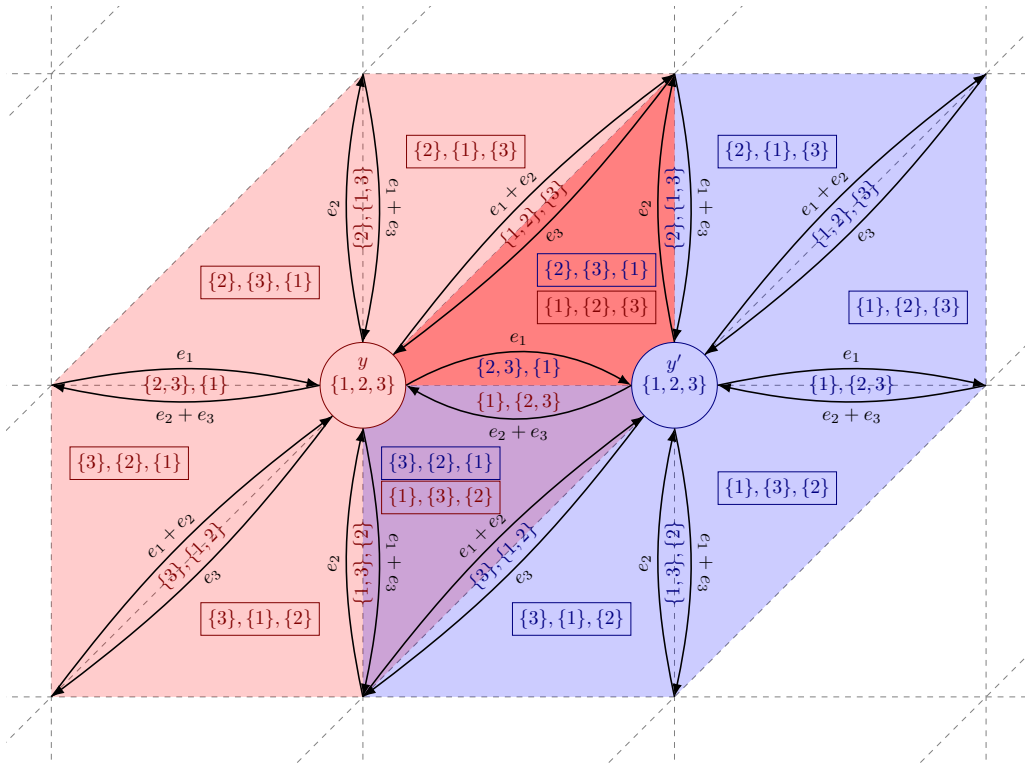
Two important facts follows. On one hand, because Coxeter and Freudenthal-Kuhn triangulations are related by an affine transformation, they have the same combinatorial structure. We call any triangulation that is the image of a Freudenthal-Kuhn triangulation under an affine transformation a CFK-triangulation. In this paper, we restrict our attention to Coxeter and Freudenthal triangulations since they are the simplest, but any CFK-triangulation could be used. The second fact is that each simplex in such a triangulation can be represented as a cell in an arrangement of $d(d-1)/2$ families of parallel hyperplanes which are known and do not need to be stored.

17:4 Isomanifold Tracing in \mathbb{R}^d , Using Coxeter-Freudenthal-Kuhn Triangulations

The next crucial observation relates CFK-triangulations and permutahedra, which allows to represent CFK-triangulations in a compact way (The definition and some combinatorial properties of permutahedra are given in [8, Appendix A]). We first recall that two complexes are dual if there is a bijection between their faces that inverses the inclusion relationships.

► **Proposition 2.** *The star of a vertex in a CFK-triangulation is combinatorially dual to a permutahedron.*

Since the facial structure of a permutahedron is fully described by ordered partitions, any simplex σ in a CFK-triangulation is characterized by a star that contains σ and by the ordered partition that specifies which simplex in the star is precisely σ . Since a simplex appears in several stars, we take the one that is centered at the lowest vertex of σ in the lexicographic order. This representation is called the permutahedral representation of a CFK-triangulation, see Figure 1. We further have:



■ **Figure 1** The permutahedral representation of the simplices in the stars of vertices y and y' .

► **Lemma 3 (Face computation).** *Let σ be an l -simplex in the FK-triangulation of \mathbb{R}^d . Computing all its k -faces can be done in time $O(ds)$, where $s = \binom{l+1}{k+1}$ is the number of k -faces of an l simplex. The space complexity of the algorithm is $O(l)$.*

► **Lemma 4 (Coface computation).** *Let σ be a k -simplex in the FK-triangulation of \mathbb{R}^d given by its permutahedral representation. Computing the permutahedral representations of all its l -cofaces can be done in time $O(ds)$, where $s \leq \frac{1}{2^{\min(l,d-l)}} \binom{d-k}{d-l} (d-k+1)!$ is the number of l -cofaces of a k -simplex in the FK-triangulation. The space complexity of the algorithm is $O(d)$.*

2.2 PL-approximation of isomanifolds

We first recall sufficient conditions under which the PL-approximation $\hat{\mathcal{M}}$ output by the algorithm faithfully reproduces the original isomanifold. These conditions are fully described in the full version of [9] and we simply state here the main results specialized to the case of CFK-triangulations.

We will say that f has *bounded complexity* if the three following quantities γ_{\max} , λ_{\min} and α_{\max} are positive and bounded.

$$\gamma_{\max} = \max_{x \in \mathcal{T}_0} (\max_i |\text{grad} f^i(x)|) \quad \lambda_{\min} = \min_{x \in \mathcal{T}_0} \lambda_{\min}(x), \quad \alpha_{\max} = \max_{x \in \mathcal{T}_0} \max_i \|\text{Hes}(f^i)(x)\|_2$$

where

- \mathcal{T}_0 denotes the set of all $\sigma \in \mathcal{T}$, such that $(f^i)^{-1}(0) \cap \sigma \neq \emptyset$ for all i .
- $\text{grad} f^i = (\partial_j f_i)_j$ denotes the gradient of component f^i , for $i \in [1, d - n]$,
- $\text{Gram}(\nabla f)$ denotes the Gram matrix whose elements are $\nabla f^i \cdot \nabla f^j$ where \cdot stands for the dot product.
- $\lambda_{\min}(x)$ denotes the smallest absolute value of the eigenvalues of $\text{Gram}(\nabla f(x))$,¹
- $\text{Hes}(f) = (\partial_k \partial_l f_i)_{k,l}$ denotes the Hessian matrix of second order derivatives,
- $|\cdot|$ denotes the Euclidean norm of a vector and $\|\cdot\|_2$ the operator 2-norm of a matrix.²

We can now restate the topological result of [9]:

► **Theorem 5.** *Assume that the function f has bounded complexity. If the precision of the CFK-triangulation satisfies $D = O(d^{-5/2})$, where the constant in the big O depends on γ_{\max} , λ_{\min} and α_{\max} , then $\hat{\mathcal{M}}$ is a manifold isotopic to the zero set \mathcal{M} of f .*

Moreover, we can bound the Fréchet distance between \mathcal{M} and $\hat{\mathcal{M}}$. The Fréchet distance is a quite strong notion of distance and, in particular, it bounds the Hausdorff distance.

► **Definition 6** (Fréchet distance for embedded manifolds). *Let \mathcal{M}_a and \mathcal{M}_b be two homeomorphic, compact submanifolds of \mathbb{R}^d . Write \mathcal{H} for the set of all homeomorphisms from \mathcal{M}_a to \mathcal{M}_b . The Fréchet distance between \mathcal{M}_a and \mathcal{M}_b is $d_F(\mathcal{M}_a, \mathcal{M}_b) = \inf_{h \in \mathcal{H}} \sup_{x \in \mathcal{M}_a} d(x, h(x))$.*

► **Theorem 7.** *Assume that the function f has bounded complexity. Then, $d_F(\mathcal{M}, \hat{\mathcal{M}}) = O(D^2)$ where the constant in the big O depends on γ_{\max} , λ_{\min} and α_{\max} .*

3 Tracing isomanifolds

In this section, we describe an algorithm that computes a PL-approximation $\hat{\mathcal{M}}$ of an isomanifold \mathcal{M} . The algorithm has some similarity with the Marching Cube algorithm [20] but departs from it in two fundamental ways. First, because of the curse of dimensionality, we cannot afford to look at all the cells in the grid and need to limit the search to cells that are close to \mathcal{M} . The problem of computing $\hat{\mathcal{M}}$ can be naturally decomposed into two subproblems: locating the various components of \mathcal{M} (i.e., finding at least one point in each connected component), and then tracing around each component, using the fact that the components are connected. This decomposition is used by various authors, see for example [27, 13]. In this paper, we focus on the tracing problem, although we discuss very briefly (Section 3.2) the problem of locating the components. As pointed out by Dobkin et al. many applications supply their own starting points.

¹ Because a Gram matrix is a symmetric square matrix, its eigenvalues are well defined and real.

² The operator norm is defined as $\|A\|_p = \max_{x \in \mathbb{R}^n} \frac{\|Ax\|_p}{\|x\|_p}$, with $\|\cdot\|_p$ the p -norm on \mathbb{R}^n .

The second major difference with the original marching cube algorithm is to replace the usual cubical grid by a CFK-triangulation of the ambient space. Taking a CFK-triangulation instead of a grid is a major advantage in high dimensions that has been recognized in the pioneering works of Allgower, and Schmidt [3] and of Dobkin et al. [13], see also [21]. The novelty here is to use the data structure of Section 2.1 to represent a CFK-triangulation. As a consequence, we will keep two main advantages of using grids: very limited storage and fast basic operations.

3.1 Isomanifolds

Let $f : \mathbb{R}^d \rightarrow \mathbb{R}^{d-n}$ be a smooth (C^2 suffices) function, and suppose that 0 is a regular value of f , meaning that at every point x such that $f(x) = 0$, the Jacobian of f is non-degenerate. Then the zero set of f is an n -dimensional manifold as a direct consequence of the implicit function theorem, see for example [14, Section 3.5]. We further assume that $f^{-1}(0)$ is compact. As in [1] we consider a triangulation \mathcal{T} of \mathbb{R}^d . The function \hat{f} is the linear interpolation of the values of f at the vertices if restricted to a single simplex $\sigma \in \mathcal{T}$, i.e.

$$\forall x \in \sigma : \hat{f}(x) = \sum_{v \in \sigma} \lambda_v(x) f(v), \quad (1)$$

where the λ_v are the barycentric coordinates of x with respect to the vertices v of σ . For any function $g : \mathbb{R}^d \rightarrow \mathbb{R}^{d-n}$ we write g^i , with $i = 1, \dots, d-n$, for the components of g .

The PL-approximation is now defined as $\hat{f}^{-1}(0) = \hat{\mathcal{M}}$. Locally, $\hat{f}|_{\sigma}^{-1}(0)$ is generically the intersection of an n -flat H_{σ} with σ . More precisely we note that $\hat{f}|_{\sigma}^{-1}(0)$ is an n -flat if the gradients of $\hat{f}^i|_{\sigma}$ are linearly independent, which can be easily achieved by perturbing f infinitesimally (or at least its values at the vertices). Let τ_j^{d-n} and τ_j^{d-n-1} be faces of σ of dimension $d-n$ and $d-n-1$. An infinitesimal perturbation of f , can prevent either $\hat{f}|_{\sigma}^{-1}(0)$ from intersecting the faces τ_j^{d-n-1} , or the gradients of $\hat{f}^i|_{\sigma}$ and the normal spaces of τ_j^{d-n} (for each fixed j) from failing to span \mathbb{R}^d . More precise statements on the geometric and topological stability of the triangulation under perturbations of f can be found in the full version of [9, Section 5]. Because $\hat{f}|_{\sigma}^{-1}(0)$ is (generically) the intersection of an n -flat (H_{σ}) and σ , it is an n -dimensional polytope denoted by C_{σ} . The PL-approximation or mesh $\hat{\mathcal{M}}$ of \mathcal{M} is the polytopal cell complex obtained by gluing the polytopes C_{σ} associated to all the simplices σ in \mathcal{T} .

3.2 Manifold tracing algorithm

Let \mathcal{M} be the zero set of some function $f : \mathbb{R}^d \rightarrow \mathbb{R}^{d-n}$, and let $\hat{\mathcal{M}}$ be the associated PL-approximation defined over a triangulation \mathcal{T} of the ambient space \mathbb{R}^d . Both n , and d are known but arbitrary, and will be considered as parameters in the complexity analysis. We write $k = d-n$ for the codimension of \mathcal{M} . The algorithm will use for \mathcal{T} a CFK-triangulation stored using the data structure from [8, Appendix A]. We assume that the manifold $\hat{\mathcal{M}}$, and the triangulation \mathcal{T} satisfy the following genericity hypothesis:

► **Hypothesis 8 (Genericity).** *Let σ be a d -simplex of \mathcal{T} that intersects H_{σ} . No subface of σ of dimension less than k intersects H_{σ} , and any subface of σ of dimension k intersects H_{σ} in at most one point and transversally.*

We note that this condition can be satisfied by an infinitesimal perturbation for isomanifolds. This requires some explanation. We recall that the CFK-triangulation is a hyperplane arrangement, and up to translation there are a finite number of k -flats that contain all

k -simplices in the CFK triangulation. Hypothesis 8 is not satisfied, if either the flat H_σ is not linearly independent of these k -flats, or if H_σ does intersect some $(k - 1)$ -flat in the CFK-triangulation. In the previous section, we have already seen that an infinitesimal perturbation ensures that H_σ is n -dimensional. Because two affine spaces whose dimensions do not add up to the ambient dimension don't intersect with genericity and two affine spaces whose dimensions add up to exactly the ambient dimension intersect in a single point, we see that genericity can be achieved by perturbing f infinitesimally. We further remark that, generically, any vertex of the PL-approximation $\hat{\mathcal{M}}$ is the intersection point between a k -simplex σ of \mathcal{T} with the n -flat H_σ that interpolates f inside σ .

■ **Algorithm 1** Manifold tracing algorithm.

```

input : the permutahedral representation of a triangulation  $\mathcal{T}$  of  $\mathbb{R}^d$ ,
         the codimension of the isomanifold  $k = d - n$ ,
         a seed  $k$ -simplex  $\tau_0$  that intersects  $\hat{\mathcal{M}}$ 
oracle : Given a  $k$ -simplex  $\sigma$  of  $\mathcal{T}$ , decide whether  $\sigma$  intersects  $H_\sigma$  and, in the
         affirmative, report the corresponding vertex  $\sigma \cap H_\sigma = \sigma \cap \hat{\mathcal{M}}$ .
output : Set  $\mathcal{S}$  of the simplices in  $\mathcal{T}$  of dimension  $k$  that intersect  $\hat{\mathcal{M}}$ , represented by
         their permutahedral representation, and the corresponding set  $\hat{\mathcal{M}}_0$  of
         intersection points
1 Initialize the queue  $\mathcal{Q}$  and the set  $\mathcal{S}$  with  $\tau_0$ 
2 while the queue  $\mathcal{Q}$  is not empty do
3   Pop a  $k$ -dimensional simplex  $\tau$  from  $\mathcal{Q}$ 
4   foreach cofacet  $\phi$  of  $\tau$  do
5     foreach facet  $\sigma$  of  $\phi$  do
6       if  $\sigma$  does not lie in  $\mathcal{S}$  and intersects  $\hat{\mathcal{M}}$  (which can be decided using the
7         oracle) then
8           Insert  $\sigma$  into the queue  $\mathcal{Q}$ 
           Insert  $\sigma$  into  $\mathcal{S}$  together with the intersection point provided by the
             oracle

```

The algorithm essentially computes the set \mathcal{S} of k -simplices of \mathcal{T} that intersect $\hat{\mathcal{M}}$. The elements of \mathcal{S} are in 1-1 correspondence with the vertices of $\hat{\mathcal{M}}$ thanks to the Genericity hypothesis. The so-called intersection oracle is a basic ingredient of the algorithm:

Intersection oracle: *Given a k -simplex σ of \mathcal{T} , decide whether σ intersects H_σ and, in the affirmative, report the corresponding vertex $\sigma \cap H_\sigma$.*

It is easy to see that the intersection oracle reduces to solving a linear system. Indeed, generically, a vertex is the intersection of a k -simplex σ of \mathcal{T} with the m -flat H_σ that interpolates f inside σ . One can compute the barycentric coordinates of $\sigma \cap H_\sigma$ by solving a linear system of k equations, and k unknowns. It then remains to check whether the barycentric coordinates are all non-negative (to ensure that the intersection point lies inside σ). It follows that the intersection oracle reduces to evaluating f at the $k + 1$ vertices of σ plus solving a $k \times k$ linear system.

In addition, we need to provide a set of k -simplices of \mathcal{T} to initialize the tracing. These simplices must intersect all the connected components of the isomanifold and are called seed simplices. If \mathcal{M} consists of multiple connected components, then a seed simplex must be provided per each connected component and we proceed in the same manner for each component. So we will assume for now that \mathcal{M} is connected.

The seed simplices are given as part of the input and we don't discuss in this paper the problem of their construction. We simply observe that they can be obtained by computing a critical point (e.g., a point with smallest x_1 -coordinate) on each connected component of the isomanifold, which reduces to finding a solution to a system of equations, on which a large body of literature exists. See for example [24, 23, 13] and also the discussion in Wenger's book [27, Section 8.4]. Once such a seed point has been computed, we simply translate and rotate the triangulation \mathcal{T} so that the seed point coincides with the barycenter of a k -simplex of \mathcal{T} and the intersection with the manifold is transversal as demanded by the genericity hypothesis (for numerical stability it is convenient if the angle between the tangent space of the manifold and the starting k -simplex is large, which is easy to ensure). If the distance between \mathcal{M} and $\hat{\mathcal{M}}$ is small enough, then $\hat{\mathcal{M}}$ also intersects the same k simplex, see Section 2.2.

The algorithm is described as Algorithm 1. It takes as input the permutahedral representation of an ambient FKC-triangulation \mathcal{T} and a seed k -simplex τ_0 of \mathcal{T} . We assume that \mathcal{T} satisfies the Genericity Hypothesis 8, which can be enforced by infinitesimal perturbations of f as discussed in Section 3.1.

The algorithm maintains the subset \mathcal{S} of the simplices in \mathcal{T} of dimension k that intersect $\hat{\mathcal{M}}$. \mathcal{S} is initialized with the seed simplex τ_0 and stored as a hash table so that we can decide in constant time if a given k -simplex belongs to \mathcal{S} . Then, starting from τ_0 , we look at all its cofacets and consider all the facets of those cofacets that are not in \mathcal{S} (i.e. they have not been considered yet). This can be done using a queue \mathcal{Q} of candidate k -simplices. Each of these simplices is queried with the intersection oracle and, if it is found to intersect $\hat{\mathcal{M}}$, it is added to \mathcal{S} if not already present. Upon termination, \mathcal{S} contains all the k -dimensional simplices of \mathcal{T} that intersect $\hat{\mathcal{M}}$. Each such intersection, which consists of a single point (by the Genericity hypothesis), is a vertex of $\hat{\mathcal{M}}$. Hence $\hat{\mathcal{M}}_0$ is the vertex set of $\hat{\mathcal{M}}$.

Note that our algorithm essentially traverses the adjacency graph of the k and $(k+1)$ -simplices of \mathcal{T} that intersect $\hat{\mathcal{M}}$. It therefore identifies not only the set $\hat{\mathcal{M}}_0$ of vertices of $\hat{\mathcal{M}}$, but also the edges joining two such vertices (associated to the cofacets of the k -simplices in \mathcal{S}). By simply reporting those cofacets on the fly, the algorithm can output the 1-skeleton $\hat{\mathcal{M}}_1$ of the n -dimensional polytopal cell complex $\hat{\mathcal{M}}$. The higher dimensional faces of $\hat{\mathcal{M}}$ are the polytopes $C_\tau = \tau \cap H_\tau$ for all the cofaces τ of the k -simplices of \mathcal{S} . If needed, the full Hasse diagram of $\hat{\mathcal{M}}$ can be computed from $\hat{\mathcal{M}}_0$. This can be done in an output sensitive manner by using the permutahedral representation of \mathcal{T} and the algorithm of [8, Appendix A] to compute cofaces by increasing dimensions.

3.3 Complexity analysis

We can easily bound the complexity of the manifold tracing algorithm as a function of the size of the output.

► **Proposition 9.** *The time complexity of the algorithm is $O(k2^n I |\mathcal{S}|)$ where I is the time complexity of one call of the intersection oracle, and $|\mathcal{S}|$ is the number of simplices of dimension k output by the algorithm.*

Since, the intersection oracle reduces to evaluating f at the $k+1$ vertices of σ plus solving a $k \times k$ linear system, $I = O(k^\omega)$ where $\omega \approx 2.375$.

We will now express the size of the output in terms of quantities that depend on the manifold, the ambient dimension d , and the resolution of the triangulation (the diameter D of a simplex) which bounds the density of the output sample, and the precision of the

approximation. Our result holds for K -sparse manifolds, i.e. submanifolds whose intersection with any k -flat consists of at most K points. In practical situations, K is usually small and, in particular, K is a constant for algebraic isomanifolds of bounded degree.

► **Proposition 10 (Size of the output).** *Assume that \mathcal{M} is contained in the unit cube $C_d = [0, 1]^d$, and that any k -flat intersects \mathcal{M} at most K times. Writing $|\mathcal{S}| = N_C$ when \mathcal{T} is a Coxeter triangulation and $|\mathcal{S}| = N_{FK}$ for a Freudenthal triangulation, we have $N_C \leq \frac{K}{n!} \times \left(\frac{d^2 \sqrt{d(d+2)}}{2\sqrt{2}D}\right)^n$ and $N_{FK} \leq \frac{K}{n!} \times \left(\frac{d^3}{\sqrt{2}D}\right)^n$ where D is the diameter of a simplex of \mathcal{T} .*

We see that Coxeter triangulations lead to smaller samples than FK-triangulations by a factor of roughly 2^n . This will be confirmed experimentally (see Figure 4).

As noticed in Section 3.2, a simple variant of the algorithm can compute the full Hasse diagram of $\hat{\mathcal{M}}$ in an output sensitive manner. The following lemma shows that the combinatorial complexity of $\hat{\mathcal{M}}$ is of the same order as the combinatorial complexity as $\hat{\mathcal{M}}_0$.

► **Proposition 11.** *The combinatorial complexity of $\hat{\mathcal{M}}$ is $|\mathcal{S}| \times \left(\frac{3}{2}\right)^n (n+1)!$, where $|\mathcal{S}|$ is bounded in Proposition 10. If $n = O(1)$, the combinatorial complexity of $\hat{\mathcal{M}}$ is polynomial in d , and $\delta = 1/D$.*

We combine Propositions 9, 10, and 11 to obtain our main result.

► **Theorem 12.** *Assume that \mathcal{M} is contained in the unit cube $[0, 1]^d$ and that any affine k -flat intersects \mathcal{M} at most K times (K is usually small, and is in particular a constant for algebraic isomanifolds of bounded degree). Let, in addition, D be the precision required on the approximation (the diameter of a simplex in the ambient triangulation \mathcal{T}). The size of the output, and the time complexity of the algorithm are polynomial in the ambient dimension d , and in $\delta = 1/D$, and exponential in the intrinsic dimension n . The same result holds for the full PL-approximation $\hat{\mathcal{M}}$ of \mathcal{M} .*

3.4 Dimensionality reduction

As seen from Proposition 10, the size $|\mathcal{S}|$ of the output of the algorithm, considered as a function of the resolution D of the triangulation, depends exponentially on n (which is to be expected), and only polynomially on d (which is fortunate). Nevertheless, the computing time of our algorithm and the size of the output depend on d . Removing the dependency on d in the time complexity is impossible since we need to evaluate a vector-valued function f at a number of points of \mathbb{R}^d , which takes $\Omega(d)$ time per evaluation. However, we will see that we can reduce the size of the mesh produced by our algorithm.

Examples of samples of \mathcal{M} whose sizes depend on n but not on d , and lead to good approximations are known. Especially important are D -nets [11, 6]. A D -net consists of a finite number of sample points of \mathcal{M} such that no point of \mathcal{M} is at distance more than D from a sample point (density condition), and no two sample points are closer than cD for some positive constant c (separation condition). A simple volume argument shows that the size of a D -net of a n -dimensional smooth submanifolds is $O(1/D^n)$ [5, Lemma 5.3]. The sample produced by our algorithm is D -dense on the piecewise linear approximation. This implies that we have a sample that has a Hausdorff distance of $D + d_F(\mathcal{M}, \hat{\mathcal{M}})$ to the manifold, where $d_F(\mathcal{M}, \hat{\mathcal{M}})$ is bounded in Theorem 7.

Since its cardinality depends on d , it is not well separated and, in particular, not a D -net of \mathcal{M} . If we are mostly interested in the output sample, we can easily sparsify it to obtain a D -net. However, by doing so, we will lose the combinatorial structure of the mesh.

17:10 Isomanifold Tracing in \mathbb{R}^d , Using Coxeter-Freudenthal-Kuhn Triangulations

We now show how to compute a D -dense sample of \mathcal{M} of size independent of d , together with a mesh. Specifically, we will reduce dimensionality using a variant of the celebrated Johnson-Lindenstrauss lemma for manifolds. Doing so, we depart from our previous worst-case analysis by allowing some approximation factor ε and tolerate a guarantee that holds only with high probability.

► **Theorem 13** (Johnson-Lindenstrauss lemma for manifolds [12, 26]). *Pick any $\varepsilon, \eta > 0$, and let $d' = \Omega\left(\frac{n}{\varepsilon^2} \log \frac{1}{\varepsilon} + \frac{1}{\varepsilon^2} \log \frac{\Gamma}{\eta}\right)$, where Γ is a quantity that depends only on intrinsic properties of \mathcal{M} . Let Φ be the projection on a random affine subspace of dimension d' . Then, with probability $> 1 - \eta$, for all $x, y \in \mathcal{M}$, we have $(1 - \varepsilon) \sqrt{\frac{d'}{d}} \leq \frac{\|\Phi x - \Phi y\|}{\|x - y\|} \leq (1 + \varepsilon) \sqrt{\frac{d'}{d}}$.*

Let $\Psi = \sqrt{\frac{d}{d'}} \Phi$. By the theorem, the image $\Psi(\mathcal{M})$ of \mathcal{M} is a submanifold of dimension n embedded in $\mathbb{R}^{d'}$. One can now run the manifold tracing algorithm in $\mathbb{R}^{d'}$ to sample, and mesh $\Psi(\mathcal{M})$. The algorithm works as described before except that we need another oracle that, given a $(d' - n)$ -simplex σ of the CFK-triangulation of $\mathbb{R}^{d'}$, decides whether its inverse image $\Psi^{-1}(\sigma)$ intersects \mathcal{M} or not. Note that $\Psi^{-1}(\sigma)$ is a $(d - d')$ -dimensional flat strip (that is the product of a face and an affine subspace) in \mathbb{R}^d , and that the complexity of this new oracle is the same as the complexity of the basic intersection oracle, i.e. polynomial in d .

Due to the scaling factor $\sqrt{d/d'}$, the resolution of the triangulation in the low dimensional space $\mathbb{R}^{d'}$ has to be scaled by the same factor if one wants to satisfy a given sampling density on \mathcal{M} . Since the geometry of the manifold is also scaled in the same way [16], the analysis of the algorithm will be unchanged. Proposition 10 then shows that the size of the output sample does not depend on d but only on n and D for fixed ε , and η . Moreover, since the complexities of the projection and of the new oracle are polynomial in d , Proposition 9 implies that the overall complexity is still polynomial in d .

3.5 Isomanifolds with boundary, and isostratifolds

The case of isomanifolds with boundary and, more generally, of isostratifolds can be handled in very much the same way. By an isomanifold of dimension n with boundary, we mean that, on top of a function $f : \mathbb{R}^d \rightarrow \mathbb{R}^{d-n}$, we are given another function $f_\partial : \mathbb{R}^d \rightarrow \mathbb{R}$, and the set we consider is $\mathcal{M} = f^{-1}(0) \cap f_\partial^{-1}([0, \infty))$. We note that $\partial\mathcal{M} = f^{-1}(0) \cap f_\partial^{-1}(0)$.

Similarly to (1), we also define $\hat{f}_\partial|_\tau(x) = \sum_{v \in \sigma} \lambda_v(x) f_\partial(v)$. We write \hat{f} for the (global) piecewise linear function that coincides with $\hat{f}|_\tau$ on each τ of \mathcal{T} , and \hat{f}_∂ for the (global) piecewise linear function that coincides with $\hat{f}_\partial|_\tau$ on each τ of \mathcal{T} . We note that the piecewise linear approximation of the boundary $\partial\hat{\mathcal{M}} = \hat{f}_\partial^{-1}(0) \cap \hat{f}^{-1}(0)$ is a subset of $\hat{f}^{-1}(0)$, i.e. the piecewise linear approximation of the manifold ignoring the boundary. The piecewise linear approximation $\hat{\mathcal{M}}$ of the manifold with boundary consists of the following cells:

- For each τ of \mathcal{T} , such that $\hat{f}_\partial|_\tau$ is positive on τ , and $(\hat{f}|_\tau)^{-1}(0) \cap \tau \neq \emptyset$, we add $(\hat{f}|_\tau)^{-1}(0) \cap \tau$.
- For each τ of \mathcal{T} , such that $(\hat{f}|_\tau)^{-1}(0) \cap \tau \neq \emptyset$, and $(\hat{f}_\partial|_\tau)^{-1}(0) \cap \tau \neq \emptyset$, we add $(\hat{f}|_\tau)^{-1}(0) \cap (\hat{f}_\partial|_\tau)^{-1}([0, \infty)) \cap \tau$.

We will assume that the Genericity Hypothesis 8 holds for both $\hat{\mathcal{M}}$, and $\partial\hat{\mathcal{M}}$.

We can now adapt the algorithm of Section 3.2 as follows. In addition to reporting the set S_k of k -faces of the triangulation \mathcal{T} that intersect $\hat{\mathcal{M}}$, the algorithm will also report the set S_{k+1} of $(k+1)$ -faces of the triangulation \mathcal{T} that intersect $\partial\hat{\mathcal{M}}$. The computation of S_{k+1} is done by the following simple modification of Algorithm 1: if the k -dimensional facet σ of τ intersects $\hat{f}^{-1}(0)$ at a point x such that $\hat{f}_\partial|_\tau(x) < 0$ (i.e. x is not in $\hat{\mathcal{M}}$), we then compute the intersection point of τ with $\hat{f}_\partial^{-1}(0)$, and put τ in S_{k+1} .

As for the case of manifolds without boundary (see the discussion at the end of Section 3.2), the algorithm traverses (and therefore computes) the 1-skeleton of $\hat{\mathcal{M}}$. Under the Genericity Hypothesis 8, the vertices of $\hat{\mathcal{M}}_1$ are in bijection with the simplices of $S_k \cup S_{k+1}$. The edges are obtained by applying the following rules below (we identify a simplex in S_k (resp. S_{k+1}) and the intersection point $S_k \cap \hat{\mathcal{M}}$ (resp. $S_{k+1} \cap \partial\hat{\mathcal{M}}$):

1. Two simplices σ_1 , and σ_2 of S_k are joined by an edge in $\hat{\mathcal{M}}_1$ if and only if there exists a simplex in \mathcal{T}_{k+1} with faces σ_1 and σ_2 .
2. Two simplices τ_1 , and τ_2 of S_{k+1} are joined by an edge in $\partial\hat{\mathcal{M}}_1$ if and only if there exists a simplex in \mathcal{T}_{k+2} with faces τ_1 and τ_2 .
3. A simplex σ of S_k , and a simplex τ of S_{k+1} are joined by an edge in $\partial\hat{\mathcal{M}}_1$ if and only if σ is a facet of τ .

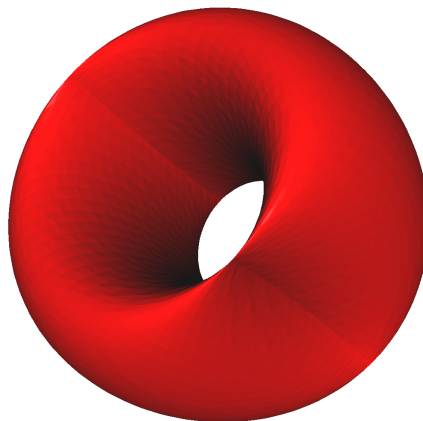
The three rules above together with the permutahedral representation of \mathcal{T} provide a way to construct the 1-skeleton of $\hat{\mathcal{M}}$ on the fly. The total cost is output sensitive. If needed, the entire combinatorial structure of $\hat{\mathcal{M}}$ can be computed by traversing the full triangulation \mathcal{T} .

The above construction generalizes easily to arbitrary isostratifolds. Isostratifolds are stratified spaces that are defined by equations and inequalities. An example of such an isostratifold is an octant of the sphere in \mathbb{R}^3 that can be defined by as $x^2 + y^2 + z^2 - 1 = 0$, $x \geq 0$, $y \geq 0$, and $z \geq 0$. We compute the 1-skeleton of $\hat{\mathcal{M}}$ and construct a graph whose nodes are the simplices of dimensions $k, k+1, \dots, d$ that intersect the strata of dimension $n, n-1, \dots, 0$.

4 Experimental results

The algorithm of Section 3 has been implemented in C++. The code is robust and fast and will be released in the GUDHI library [18]. Full detail on the implementation, including the implementation of the oracle, can be found in [19].

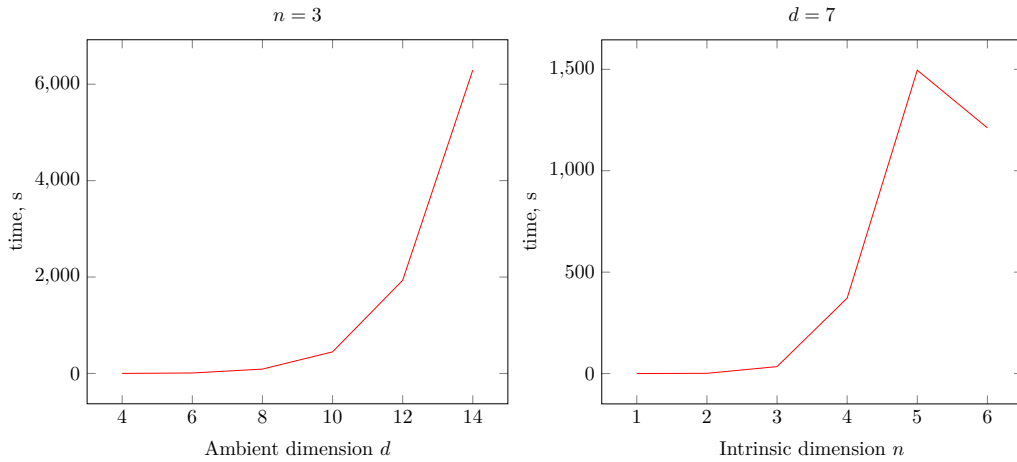
In this section, we explore the dependency of our C++ implementation of the data structure for the ambient CFK-triangulation, and of the manifold tracing algorithm on the properties of the triangulation, and of the input manifold.



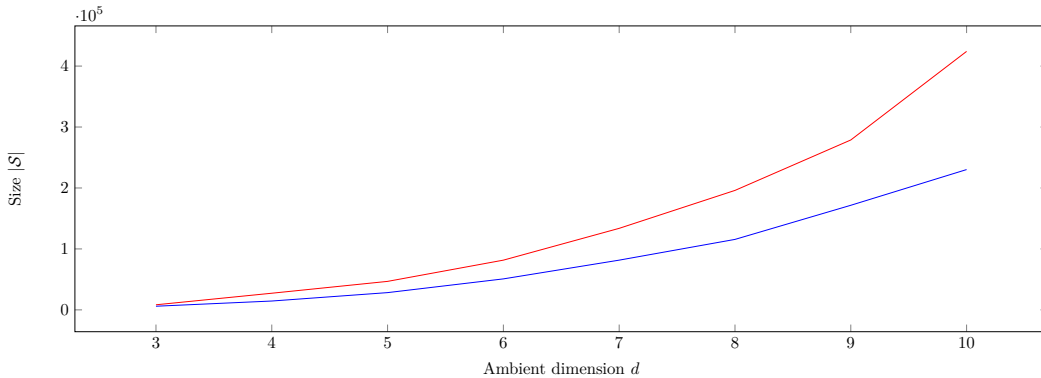
■ **Figure 2** The piecewise-linear approximation of a flat torus embedded in \mathbb{R}^{10} defined by the equations $x_1^2 + x_2^2 = 1$, and $x_3^2 + x_4^2 = 1$, and $x_i = 0$ for $i > 4$, projected to \mathbb{R}^3 . The ambient triangulation used is a Coxeter triangulation of type \tilde{A}_{10} with the diameter of the full-dimensional simplices 0.23. The output size $|\mathcal{S}|$ is 509 952. The execution time of the algorithm is 231s. The torus has been rotated and translated in \mathbb{R}^{10} so that the coordinate axes do not play any special role.

4.1 Performance of the algorithm

We show the performance of our implementation of the manifold tracing algorithm for various ambient and intrinsic dimensions in Figure 3. In Figure 4, we can see that using Coxeter triangulation is beneficial in practice as it produces a smaller output in less time (see Proposition 10).



■ **Figure 3** The effect of the ambient dimension d and of the intrinsic dimension n on the computation time of the manifold tracing algorithm. The reconstructed manifold in the tests is the n -dimensional sphere embedded in \mathbb{R}^d . The ambient triangulation used is a Coxeter triangulation of type \tilde{A}_d . The diameter of the full simplices is fixed for all d .

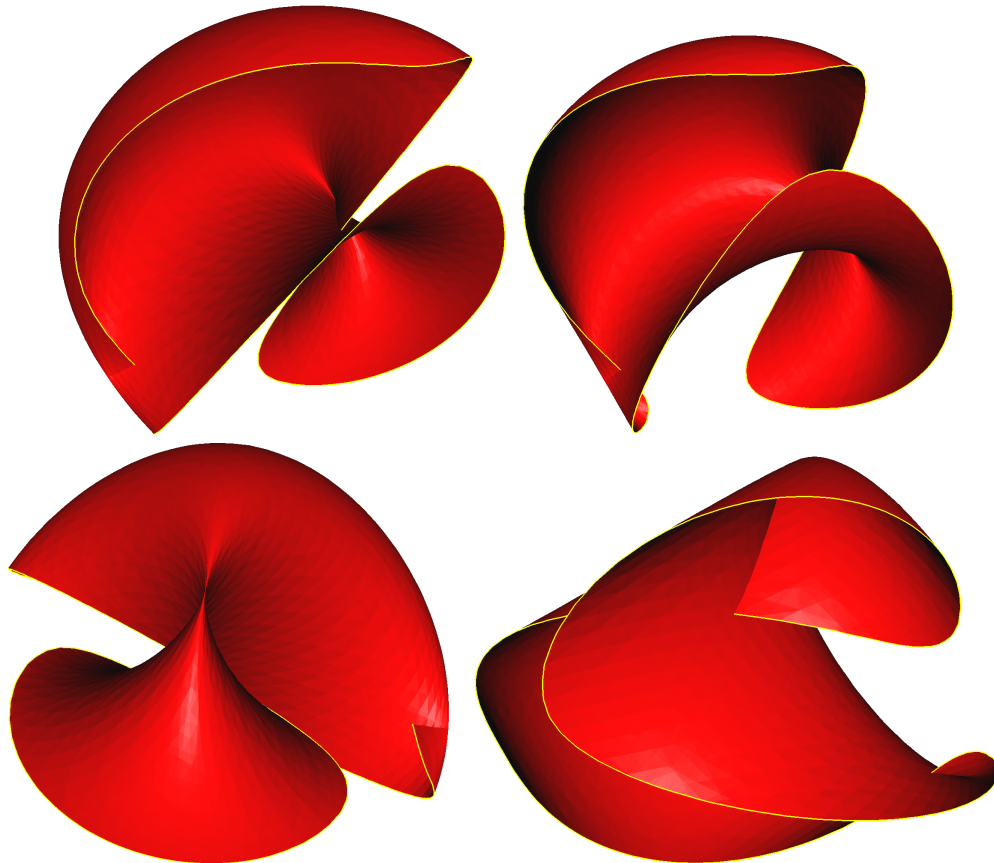


■ **Figure 4** Comparison of the size of the output of the manifold tracing algorithm using two types of ambient triangulations: a Coxeter triangulation of type \tilde{A}_d (in blue), and the Freudenthal-Kuhn triangulation of \mathbb{R}^d (in red) with the same diameter $0.07\sqrt{d}$ of d -dimensional simplices. The reconstructed manifold is the 2-dimensional implicit surface “Chair” embedded in \mathbb{R}^d given by the equations: $(x_1^2 + x_2^2 + x_3^2 - 0.8)^2 - 0.4((x_3 - 1)^2 - 2x_1^2)((x_3 + 1)^2 - 2x_2^2) = 0$, and $x_i = 0$ for $i > 3$.

In Figure 2, we present a PL approximation of a two-dimensional Clifford torus without boundary embedded in \mathbb{R}^{10} built by the manifold tracing algorithm. The torus has been rotated and translated in \mathbb{R}^{10} so that the coordinate axes do not play any special role. Note that there is no C^2 isometric embedding of the Clifford torus in \mathbb{R}^3 .

4.2 Manifolds with boundary

The algorithm has been adapted to handle submanifolds with boundary and surfaces with a piecewise smooth boundary, see Section 3.5. In Figure 5, we present the mesh obtained by our algorithm on a portion of a flat torus embedded in \mathbb{R}^4 , and cut by a hypersphere. The torus has been rotated and translated in \mathbb{R}^4 so that the coordinate axes do not play any special role.



■ **Figure 5** Four views of the flat torus in \mathbb{R}^4 given by two equations $x_1^2 + x_2^2 = 1$, and $x_3^2 + x_4^2 = 1$ cut by the hypersphere $(x_1 - 1)^2 + x_2^2 + (x_3 - 1)^2 + x_4^2 = 4$, projected to \mathbb{R}^3 . The ambient triangulation used is a Coxeter triangulation of type A_4 with the diameter 0.15 of the full-dimensional simplices. The reconstructed boundary is highlighted in yellow. The size $|\mathcal{S}|$ of the piecewise-linear approximation is 14 779. The execution time of the algorithm is 1.84s. The torus has been rotated and translated in \mathbb{R}^4 so that the coordinate axes do not play any special role.

4.3 An application in algebraic geometry

We also applied our algorithm to a more complicated example of interest in algebraic geometry [4] where an active field of research is to understand the geometry and topology of various projective varieties. Projective varieties are isomanifolds defined by polynomial equations in the complex projective space $\mathbb{C}\mathbb{P}^d = (\mathbb{C}^{d+1} \setminus 0) / \mathbb{C}^*$ of complex dimension d . One such example is the complex one-dimensional curve (that is a real dimensional surface) given by the equation $z_1^2 \bar{z}_2 + z_2^2 \bar{z}_3 + z_3^2 \bar{z}_1 = 0$ in $\mathbb{C}\mathbb{P}^2$, where \bar{z} denotes the conjugate of the complex number z .

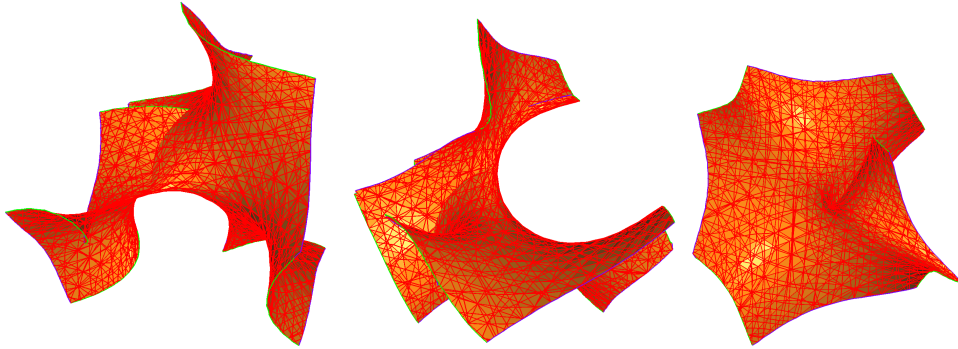
17:14 Isomanifold Tracing in \mathbb{R}^d , Using Coxeter-Freudenthal-Kuhn Triangulations

To be able to apply our algorithm, we first need to pass from homogenous coordinates $[z_1 : \dots : z_{d+1}]$ on \mathbb{CP}^d to affine coordinates $[z'_1 : \dots : z'_{i-1} : 1 : z'_{i+1} : \dots : z'_{d+1}]$ by picking the i th coordinate to be equal to 1, that is $z'_j = z_j/z_i$. Given some homogenous coordinates $[z_1 : \dots : z_{d+1}]$, we can choose the i th coordinate to be set to 1 to be the coordinate whose absolute value is the largest, so that \mathbb{CP}^d can be written as the union of the $d + 1$ sets $\{[z'_1 : \dots : z'_{i-1} : 1 : z'_{i+1} : \dots : z'_{d+1}] \mid |z'_j| \leq 1\}$, with the boundaries of these sets identified. Writing $z'_j = x_j + iy_j$ these sets are (seen as real sets) identical to the domain of \mathbb{R}^{2d}

$$D_i = \{(x_1, y_1, \dots, x_{i-1}, y_{i-1}, x_{i+1}, y_{i+1}, \dots, x_{d+1}, y_{d+1}) \mid x_j^2 + y_j^2 \leq 1\}.$$

Let f be a homogenous polynomial in $d+1$ complex variables and their complex conjugates. For each i , we can fix the i th coordinate to be 1. Writing each variable in terms of its real and imaginary part yields a real inhomogeneous polynomial in $2d$ (real) variables on the domain D_i . Taking the real and imaginary parts of the function yields two real functions $f_{\Re,i}$ and $f_{\Im,i}$ on D_i . As real sets, the projective variety $f = 0$ on \mathbb{CP}^d and the intersection of the sets $f_{\Re,i} = 0$ and $f_{\Im,i} = 0$ on D_i for each i (with the boundaries identified) are the same. We can therefore apply the tracing algorithm to each isomanifold ($f_{\Re,i} = 0, f_{\Im,i} = 0$) of D_i independently. Since their boundaries coincide, we can then glue these isomanifolds along their boundary to obtain a PL-approximation of the projective variety $f = 0$. This, for example, allows to recover the Euler characteristic of $f = 0$ on \mathbb{CP}^d .

This principle generalizes to varieties of higher codimension, that is to varieties defined by a number of homogenous polynomials f_1, \dots, f_{d-m} .



■ **Figure 6** The three triangulated surfaces as discussed in the example of $z_1^2 \bar{z}_2 + z_2^2 \bar{z}_3 + z_3^2 \bar{z}_1 = 0$ in \mathbb{CP}^2 after projection from \mathbb{R}^4 to \mathbb{R}^3 .

We illustrate the above construction on the above equation $z_1^2 \bar{z}_2 + z_2^2 \bar{z}_3 + z_3^2 \bar{z}_1 = 0$ in \mathbb{CP}^2 . By passing to affine coordinates, we recover $z_1^2 \bar{z}_2 + z_2^2 + \bar{z}_1 = 0$, $z_1^2 + \bar{z}_3 + z_3^2 \bar{z}_1 = 0$, and $\bar{z}_2 + z_2^2 \bar{z}_3 + z_3^2 = 0$. By expanding $z_1 = x_1 + iy_1$, $z_2 = x_2 + iy_2$, and $z_3 = x_3 + iy_3$, we find two real equations for each of the complex equations. We give those corresponding to $z_1^2 \bar{z}_2 + z_2^2 + \bar{z}_1 = 0$, the other equations being symmetric. For this complex equation, we get the real equations $x_1 + x_1^2 x_2 + x_2^2 - x_2 y_1^2 + 2x_1 y_1 y_2 - y_2^2 = 0$ and $-y_1 + 2x_1 x_2 y_1 - x_1^2 y_2 + 2x_2 y_2 + y_1^2 y_2 = 0$ in \mathbb{R}^4 . The domain D_3 is in this case determined by the equations $x_1^2 + y_1^2 \leq 1$ and $x_2^2 + y_2^2 \leq 1$. Hence we find a surface in \mathbb{R}^4 with a piecewise smooth boundary. The result provided by our algorithm is shown in Figure 6. For visualization purposes, we show the three surfaces separately and projected from \mathbb{R}^4 to \mathbb{R}^3 .

5 Conclusion and open questions

We have presented an efficient, practical and provably correct algorithm to compute the PL-approximation of an isomanifold of any dimension and codimension. Since isomanifolds are a special type of manifolds, it is tempting to see if our algorithm extends to general smooth submanifolds of \mathbb{R}^d .

The manifold tracing algorithm itself is quite general and works for any submanifold as soon as we provide a seed point and an oracle that can determine whether a k -simplex of the ambient triangulation intersects \mathcal{M} or not. In this general setting, the simple algorithm described above is sufficient to compute a PL-approximation of the manifold and satisfies the bounds given in Section 3.

However, this is not enough to obtain guarantees on the geometric and topological quality of the output mesh. Such guarantees can be obtained by slightly perturbing the ambient Coxeter triangulation of type \tilde{A}_d so that the following conditions are satisfied:

1. All k -dimensional faces τ in \mathcal{T} , with $k \leq d - n - 1$, are far enough from \mathcal{M} .
2. The longest edge length of \mathcal{T} is upper bounded and its smallest thickness is lower bounded.

Under these conditions, Algorithm 1 will output a PL-approximation that is topologically equivalent and close in Hausdorff distance to the input manifold [7]. However, the perturbation scheme of [7] perturbs (in the worst case) all the simplices of \mathcal{T} of dimension less than the codimension $d - n$ that are incident on a vertex (in a neighbourhood of \mathcal{M}). Since there are exponentially many such simplices, such methods have a complexity that depends exponentially on the ambient dimension d , and have not proved useful in practice except in some simple cases. It remains open whether general smooth manifolds embedded in \mathbb{R}^d can be triangulated in time polynomial in d as we were able to do here in the special case of isomanifolds.

References

- 1 Eugene Allgower and Kurt Georg. Estimates for piecewise linear approximations of implicitly defined manifolds. *Applied Mathematics Letters*, 2(2):111–115, 1989. doi:10.1016/0893-9659(89)90001-3.
- 2 Eugene Allgower and Kurt Georg. *Numerical continuation methods: an introduction*, volume 13. Springer Science & Business Media, 1990. doi:10.1007/978-3-642-61257-2.
- 3 Eugene Allgower and Phillip H. Schmidt. An algorithm for piecewise-linear approximation of an implicitly defined manifold. *SIAM Journal on Numerical Analysis*, 22(2):322–346, 1985. doi:10.1137/0722020.
- 4 Aurélien Alvarez and Bertrand Deroin. Dynamique et topologie du feuilletage de Jouanolou. Preprint, 2019.
- 5 Jean-Daniel Boissonnat, Frédéric Chazal, and Mariette Yvinec. *Geometric and Topological Inference*. Cambridge Texts in Applied Mathematics. Cambridge University Press, 2018. doi:10.1017/9781108297806.
- 6 Jean-Daniel Boissonnat and Arijit Ghosh. Manifold reconstruction using tangential Delaunay complexes. *Discrete & Computational Geometry*, 51(1):221–267, 2014. doi:10.1007/s00454-013-9557-2.
- 7 Jean-Daniel Boissonnat, Siargey Kachanovich, and Mathijs Wintraecken. Triangulating submanifolds: An elementary and quantified version of Whitney’s method. *Discrete & Computational Geometry*, pages 1–49, 2020. doi:10.1007/s00454-020-00250-8.
- 8 Jean-Daniel Boissonnat, Siargey Kachanovich, and Mathijs Wintraecken. Tracing Isomanifolds in \mathbb{R}^d in Time Polynomial in d using Coxeter-Freudenthal-Kuhn Triangulations. Full version of this paper, 2021. URL: <https://hal.inria.fr/hal-03006663>.

- 9 Jean-Daniel Boissonnat and Mathijs Wintraecken. The topological correctness of PL-approximations of isomanifolds. In *34th International Symposium on Computational Geometry, SoCG 2020, June 23-26, 2020, Zurich, Switzerland.*, 2020. Full version. URL: <https://hal.inria.fr/hal-02386193>.
- 10 Yen-Chi Chen. Solution manifold and its statistical applications, 2020. arXiv:2002.05297. arXiv:2002.05297.
- 11 Siu-Wing Cheng, Tamal K Dey, and Edgar A Ramos. Manifold reconstruction from point samples. In *SODA*, pages 1018–1027, 2005.
- 12 Kenneth L. Clarkson. Tighter bounds for random projections of manifolds. In *Proceedings of the 24th ACM Symposium on Computational Geometry, College Park, MD, USA, June 9-11, 2008*, pages 39–48, 2008. doi:10.1145/1377676.1377685.
- 13 David P. Dobkin, Allan R. Wilks, Silvio V. F. Levy, and William P. Thurston. Contour tracing by piecewise linear approximations. *ACM Transactions on Graphics (TOG)*, 9(4):389–423, 1990. doi:10.1145/88560.88575.
- 14 J. J. Duistermaat and J. A. C. Kolk. *Multidimensional Real Analysis I: Differentiation*. Number 86 in Cambridge Studies in Advanced Mathematics. Cambridge University Press, 2004. doi:10.1017/CB09780511616716.
- 15 B. Curtis Eaves. *A course in triangulations for solving equations with deformations*, volume 234. Lecture Notes in Economics and Mathematical Systems, 1984. doi:10.1007/978-3-642-46516-1.
- 16 Armin Eftekhari and Michael B. Wakin. What happens to a manifold under a bi-Lipschitz map? *Discrete & Computational Geometry*, 57(3):641–673, 2017. doi:10.1007/s00454-016-9847-6.
- 17 A. Gomes, I. Voiculescu, J. Jorge, B. Wyvill, and C. Galbraith. *Implicit Curves and Surfaces: Mathematics, Data Structures and Algorithms*. Springer, 2009. doi:10.1007/978-1-84882-406-5.
- 18 GUDHI Project. URL: <http://gudhi.gforge.inria.fr/doc/latest/>.
- 19 Siargey Kachanovich. *Meshing submanifolds using Coxeter triangulations*. Theses, COMUE Université Côte d’Azur (2015 - 2019), 2019. URL: <https://hal.inria.fr/tel-02419148>.
- 20 William E. Lorensen and Harvey E. Cline. Marching cubes: A high resolution 3d surface construction algorithm. *ACM siggraph computer graphics*, 21(4):163–169, 1987. doi:10.1145/37401.37422.
- 21 Chohong Min. Simplicial isosurfacing in arbitrary dimension and codimension. *Journal of Computational Physics*, 190(1):295–310, 2003. doi:10.1016/S0021-9991(03)00275-4.
- 22 Timothy S. Newman and Hong Yi. A survey of the marching cubes algorithm. *Computers & Graphics*, 30(5):854–879, 2006. doi:10.1016/j.cag.2006.07.021.
- 23 James M Ortega and Werner C Rheinboldt. *Iterative solution of nonlinear equations in several variables*. Classics in Applied Mathematics. SIAM, 2000. doi:10.1137/1.9780898719468.
- 24 Alexander M Ostrowski. *Solution of Equations and Systems of Equations: Pure and Applied Mathematics: A Series of Monographs and Textbooks, Vol. 9*, volume 9. Elsevier, 2016.
- 25 Michael J. Todd. *The computation of fixed points and applications*, volume 124. Lecture Notes in Economics and Mathematical Systems, 1976. doi:10.1007/978-3-642-50327-6.
- 26 Nakul Verma. A note on random projections for preserving paths on a manifold. Technical Report Tech. Report CS2011-0971, UC San Diego, 2011.
- 27 Rephael Wenger. *Isosurfaces: geometry, topology, and algorithms*. AK Peters/CRC Press, 2013.
- 28 H. Whitney. *Geometric Integration Theory*. Princeton University Press, 1957. doi:10.1515/9781400877577.